Middle Miocene climate cooling linked to intensification of eastern equatorial Pacific upwelling

Ann Holbourn[1]*, Wolfgang Kuhnt[1], Mitch Lyle[2], Leah Schneider[3], Oscar Romero[4], and Nils Andersen[5]
[1]Institute of Geosciences, Christian-Albrechts-University, D-24118 Kiel, Germany
[2]Department of Oceanography, Texas A&M University, TAMU 3146, College Station, Texas 77840-3146, USA
[3]Integrated Ocean Drilling Program, Department of Geology and Geophysics, Texas A&M University, 1000 Discovery Drive, College Station, Texas 77845, USA
[4]Instituto Andaluz de Ciencias de la Tierra (CSIC-UGR), Avenida de las Palmeras 4, 18100 Armilla-Granada, Spain
[5]Leibniz Laboratory for Radiometric Dating and Stable Isotope Research, Christian-Albrechts-University, D-24118 Kiel, Germany

ABSTRACT

During the Middle Miocene, Earth's climate transitioned from a relatively warm phase (Miocene climatic optimum) to a colder mode with reestablishment of permanent ice sheets on Antarctica, thus marking a fundamental step in Cenozoic cooling. Carbon sequestration and atmospheric CO_2 drawdown through increased terrestrial and/or marine productivity have been proposed as the main drivers of this fundamental transition. We integrate high-resolution (1–3 k.y.) benthic stable isotope data with X-ray fluorescence scanner–derived biogenic silica and carbonate accumulation estimates in an exceptionally well preserved sedimentary archive, recovered at Integrated Ocean Drilling Program Site U1338, to reconstruct eastern equatorial Pacific productivity variations and to investigate temporal links between high- and low-latitude climate change over the interval 16–13 Ma. Our records show that the climatic optimum (16.8–14.7 Ma) was characterized by high-amplitude climate variations, marked by intense perturbations of the carbon cycle. Episodes of peak warmth at (Southern Hemisphere) insolation maxima coincided with transient shoaling of the carbonate compensation depth and enhanced carbonate dissolution in the deep ocean. A switch to obliquity-paced climate variability after 14.7 Ma concurred with a general improvement in carbonate preservation and the onset of stepwise global cooling, culminating with extensive ice growth over Antarctica ca. 13.8 Ma. We find that two massive increases in opal accumulation ca. 14.0 and ca. 13.8 Ma occurred just before and during the final and most prominent cooling step, supporting the hypothesis that enhanced siliceous productivity in the eastern equatorial Pacific contributed to CO_2 drawdown.

INTRODUCTION

The Miocene climatic optimum (MCO, ca. 17–15 Ma) represents a prolonged, geologically recent interval of global warmth that provides a useful analogue for projections of a future warmer Earth. However, the MCO remains an enigmatic episode in Earth's climate history, and comparatively little is known about the processes sustaining global warmth and about the chain of climate events that reversed this trend and promoted ice growth on Antarctica after ca. 15 Ma. Hypotheses concerning the cause and end of the MCO have focused on changing atmospheric pCO_2 concentrations, and most scenarios invoked carbon sequestration ending Middle Miocene global warmth (Vincent and Berger, 1985; Woodruff and Savin, 1991; Flower and Kennett, 1994; Holbourn et al., 2005; Shevenell et al., 2008; Badger et al., 2013). Unfortunately, deep-time pCO_2 reconstructions still present major challenges, and the time scales on which CO_2 drawdown and climate change occurred, as well as the locations of major carbon sinks in the Miocene, remain unclear. Understanding this major step in Earth's evolution is nevertheless crucial to explore the full spectrum of natural variability and to untangle dynamical processes and feedbacks controlling climate evolution over multiple time scales.

Drilling at Integrated Ocean Drilling Program (IODP) Site U1338 (2°30.469′N, 117°58.178′W; 4200 m water depth, backtracked to ~3000–3500 m Middle Miocene water depth; Pälike et al., 2012) recently recovered a continuous carbonate-rich Middle Miocene succession from the eastern equatorial Pacific (EEP, Fig. 1). This region plays a key role in regulating global climate, as it traps a vast amount of solar radiation, is a major area of high primary productivity (Chavez and Barber, 1987; Westberry et al., 2008), and is a locus of CO_2 exchange between the ocean and atmosphere (Takahashi et al., 1997). The EEP biogenic sediments provide an exceptional archive of fundamental changes in primary productivity, ice volume, and oceanic circulation since ca. 16 Ma (Lyle et al., 1995, 2008; Pälike et al., 2010, 2012). We present astronomically tuned benthic stable isotope records (~1–3 k.y. time resolution) that track climate evolution in unprecedented resolution over the later part of the MCO and through the transition to a glaciated mode with permanent polar ice (Fig. 2; Figs. DR1 and DR2 in the GSA Data Repository[1]). We combine these new records with X-ray fluorescence scanner–derived elemental records (Lyle et al., 2012) and biogenic silica data to reconstruct temporal variations in carbonate and silica fluxes, to monitor changes in equatorial productivity, and to evaluate high- to low-latitude teleconnections.

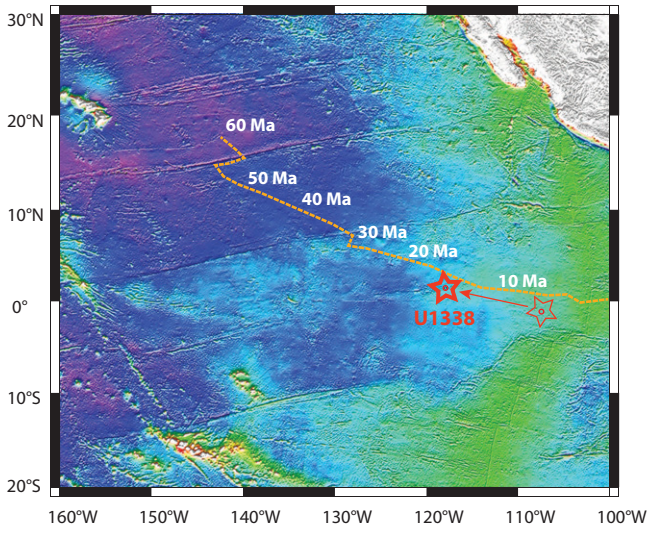

Figure 1. Map showing location of Integrated Ocean Drilling Program Site U1338 with backtracked position of paleoequator. Thin star indicates backtracked position of site at crustal age 16 Ma (simplified from Pälike et al., 2010).

*E-mail: ah@gpi.uni-kiel.de.

[1]GSA Data Repository item 2014005, methods and supplementary Figures DR1–DR4, is available online at www.geosociety.org/pubs/ft2014.htm, or on request from editing@geosociety.org or Documents Secretary, GSA, P.O. Box 9140, Boulder, CO 80301, USA.

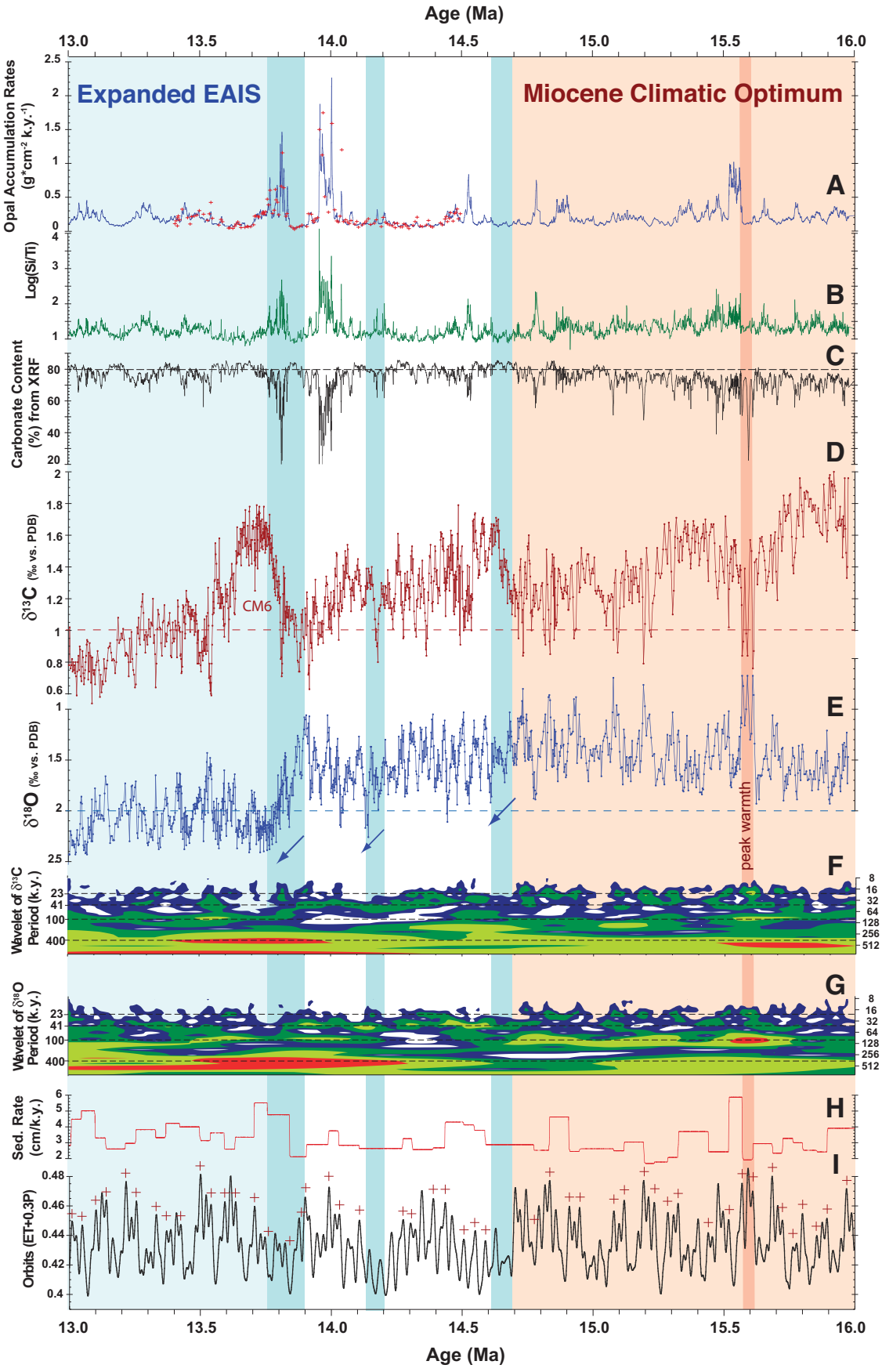

Figure 2. Paleoceanographic records (1.5–3 k.y. time resolution) from Integrated Ocean Drilling Program (IODP) Site U1338, spanning later part of Miocene climatic optimum and transition into glacial climate mode. A: Opal accumulation rates from X-ray fluorescence (XRF) scanner (blue line) and from opal measurements (red crosses). B: Silica content expressed as log(Si/Ti) (from Lyle et al., 2012). C: Carbonate percentages calculated from X-ray fluorescence (XRF) scanner and gamma ray attenuation porosity evaluation density data (from Lyle et al., 2012). Dashed line indicates 80% $CaCO_3$. D: Benthic foraminiferal $\delta^{13}C$. CM6 represents last and most prominent 400 k.y. $\delta^{13}C$ maximum of Monterey Excursion. PBD—Peedee belemnite. E: Benthic foraminiferal $\delta^{18}O$. F: Wavelet power spectrum of $\delta^{13}C$ time series. Dashed lines indicate main Milankovitch periodicities 23 k.y., 41 k.y., 100 k.y., and 400 k.y. G: Wavelet power spectrum of $\delta^{18}O$ time series. Dashed lines indicate main Milankovitch periodicities 23 k.y., 41 k.y., 100 k.y., and 400 k.y. H: Sedimentation (Sed.) rates. I: Eccentricity-tilt-precession tuning target (ET + 0.3P; from Laskar et al., 2004). Crosses indicate age correlation points. Blue bars and arrows mark major $\delta^{18}O$ increases associated with high-latitude cooling; orange bar marks extreme $\delta^{18}O$ minima possibly associated with pulse of intense warming on Antarctica (Warny et al., 2009). EAIS—East Antarctic Ice Sheet.

METHODS

We measured $\delta^{18}O$ and $\delta^{13}C$ in the epifaunal benthic foraminifers *Planulina wuellerstorfi* or *Cibicidoides mundulus* in ~5–10 cm intervals (for detailed methods, see Holbourn et al., 2007). Data sets are archived at the World Data Center for Marine Environmental Sciences (WDC-MARE, http://doi.pangaea.de/10.1594/PANGAEA.8200095). Building on the shipboard stratigraphy, we developed a new chronology by correlating the benthic foraminiferal $\delta^{18}O$ series to computed variations of the Earth's orbit (Laskar et al., 2004). As a tuning target, we constructed an eccentricity-tilt-precession composite with no phase shift and with equal weight of eccentricity and obliquity and only 1/3 precession. We correlated $\delta^{18}O$ minima to eccentricity-tilt-precession maxima, following a minimal tuning approach to preserve original spectral characteristics. The independently tuned Site U1338 isotope data correlate well with astronomically tuned $\delta^{18}O$ and $\delta^{13}C$ records from the southeast and northwest subtropical Pacific (Holbourn et al., 2007). For methods for opal (biogenic silica) measurement, and calculation of accumulation rates, see the Data Repository.

MIOCENE CLIMATE OPTIMUM

High-Amplitude Climate Variability

Our benthic stable isotope data demonstrate that the MCO was characterized by high-amplitude climate variability (Fig. 2; Fig. DR3). This is particularly striking within the interval 15.7–14.7 Ma, when $\delta^{18}O$ fluctuated between 1.9‰ and 0.7‰, and $\delta^{13}C$ varied between 1.7‰ and 0.7‰, respectively. Nine intense global warming pulses ($\delta^{18}O$ decreases), which coincide with sharp negative shifts in $\delta^{13}C$, are paced by 100 k.y. eccentricity. The most intense of the $\delta^{18}O$ minima between 15.7 and 14.7 Ma are generally marked by minima in carbonate content, and minima in sediment coarse fraction >63 µm. The correlation between carbonate content and $\delta^{18}O$ disappears after ca. 14.7 Ma, and carbonate preservation generally improves after the end of the MCO.

The Site U1338 records support that deep-ocean carbonate dissolution increased, as the lysocline shoaled during the warmest episodes of the MCO ($\delta^{18}O$ reaching ~1‰ or less). Transient warmings concur with increases in log(Ti/Ca) and log(Al/Ca) and with decreases in the coarse residue and in sedimentation rates, indicating enhanced carbonate dissolution (Fig. DR3). Log(Si/Ti), regarded here as a proxy of opal production and deposition, does not show any marked increase during warm intervals, indicating that increases in log(Si/Ca) were mainly driven by carbonate dissolution during the MCO. The Site U1338 carbonate dissolution pattern is in agreement with proxy records from Ocean Drilling Program (ODP) Site 1237 (Holbourn et al., 2007), located at comparable paleodepth in the subtropical southeast Pacific, which supports that eccentricity-paced carbonate dissolution cycles were an ocean-wide feature during the MCO.

Processes Driving MCO Climate Variations

The prominent 100 k.y. $\delta^{18}O$ cycles characterizing the MCO differ markedly from the characteristic saw-toothed shape of the late Pleistocene glacial cycles. The MCO cycles are more symmetrical, with sharp decreases and increases, implying that different climate dynamics drove these events (Fig. 1; Fig. DR3). Such high-amplitude $\delta^{18}O$ fluctuations cannot be solely attributed to rapid waxing and waning of an unstable Antarctic ice shield, but must also reflect major changes in deep and intermediate water temperature. Because these fluctuations are recorded at different water depths and in several ocean basins (Woodruff and Savin, 1991), they cannot be ascribed to shifts in water mass boundaries, but must relate to global climate and circulation changes. The relatively rapid recovery in $\delta^{13}C$ (0.1‰ to 0.15‰ per k.y.) following MCO warm events supports that fluctuations in productivity and organic carbon burial were involved rather than long-term shifts in rates of weathering or in the shelf carbonate reservoir, typically associated with large-scale sea-level fall or rise. The most striking of the MCO transient warmings is the abrupt $\delta^{18}O$ decrease centered ca. 15.6 Ma, which corresponds to a deep-water warming of ~5 °C, assuming that little ice volume change occurred. The high-resolution data from Site U1338 reveal that this extreme $\delta^{18}O$ event carries a strong precessional signal (Fig. 1; Fig. DR3), supporting a contributing role for insolation as a trigger of intense warming events during the MCO.

CLIMATE COOLING LINKED TO UPWELLING INTENSIFICATION

From ca. 14.7 Ma, a new pattern of climate variability emerges with dampening of the benthic $\delta^{18}O$ signal and shortening of the dominant rhythm from 100 to 41 k.y. (Fig. 1). This change also concurs with a general improvement in carbonate preservation. A salient feature of the $\delta^{18}O$ record is the massive increase at 13.9–13.8 Ma that has been attributed to Antarctic ice-sheet expansion and deep-water cooling (Shackleton and Kennett, 1975; Miller et al., 1991; Woodruff and Savin, 1991; Flower and Kennett, 1994; Holbourn et al., 2005; Shevenell et al., 2008) and coincides with the onset of the last and most prominent 400 k.y. $\delta^{13}C$ maximum of the Monterey Excursion (CM6). Several lines of evidence support an intensification of equatorial upwelling linked to high-latitude cooling ($\delta^{18}O$ increases), both prior to and during the major ice expansion at 13.9–13.8 Ma. First, massive spikes in Site U1338 log(Si/Ti), reflecting maxima in opal accumulation rates, occur during colder intervals between 14.04 and 13.96 Ma and between 13.84 and 13.76 Ma (Fig. 2). These prominent opal increases concur with transient drops in benthic $\delta^{13}C$, providing evidence of a more active biological pump as a result of a substantial increase in EEP primary production. Second, sedimentation rates are relatively high during these intervals, indicating low carbonate dissolution, thereby corroborating high siliceous productivity in surface waters and elevated opal accumulation rates. Lower resolution alkenone-derived sea surface temperatures exhibit a marked transient cooling ca. 13.8 Ma (Rousselle et al., 2013), supporting intensified upwelling of cooler waters to the ocean surface at that time.

Silica acts as a main limiting nutrient in equatorial upwelling areas, as its availability controls diatom production (Dugdale and Wilkerson, 1998; Ragueneau et al., 2000). When the supply of silica increases, diatoms normally outcompete other primary producers, including coccolithophorids (Ragueneau et al., 2000). The close coupling between increased productivity and heavier benthic $\delta^{18}O$ suggests a link to high-latitude cooling through increased advection of Si-rich waters toward the low latitudes during colder phases. A sharper latitudinal thermal gradient may also have led to intensification of convective atmospheric circulation in the low latitudes, increasing delivery of dust to the upper ocean and shoaling of the thermocline, thereby promoting upwelling of nutrient-rich waters within the EEP. Similar controls have been proposed to explain climatic responses to obliquity promoting more persistent La Niña–like conditions during colder Pliocene periods (Philander and Fedorov, 2003; Fedorov et al., 2006; Lawrence et al., 2006).

Our results suggest that the emergence of the Pacific cold tongue played a role in fostering CO_2 drawdown and climate cooling, as the EEP evolved from being a CO_2 contributor during the MCO to becoming a carbon sink. Today the cold tongue is a net contributor of CO_2 to the atmosphere because primary productivity is limited by silica and iron availability (Takahashi et al., 1997; Dugdale and Wilkerson, 1998). Consequently, the carbon export to the deep sea does not compensate the outgassing of CO_2 from upwelling. However, during the last glacial period, silica leakage from the southern high latitudes and increased delivery of dust-blown iron to the EEP may have promoted carbon export and contributed to lower atmospheric pCO_2 (Winckler et al., 2008; Pichevin et al., 2009). Estimated opal accumulation rates over the 2 intervals of enhanced primary productivity between 14.04 and 13.96 Ma and between 13.84 and 13.76 Ma are substantially higher than Pleistocene glacial rates. Typical opal mass accumulation rates for the Pleistocene EEP are ~0.1–0.2 g/cm^2/k.y. (Lyle et al., 1988), close to Middle Miocene background rates (Fig. 2). In contrast,

at the peak of the Middle Miocene high productivity events, opal burial was more than one order of magnitude higher than background values.

It is interesting that the first opal pulse ca. 14 Ma preceded the major climate transition, suggesting preconditioning of the climate system, possibly linked to renewed high-amplitude 100 k.y. eccentricity forcing after 14.1 Ma. During the second opal pulse, positive feedbacks associated with intensified productivity and CO_2 drawdown in the EEP at Southern Hemisphere insolation minima probably accentuated the cooling trend. Our results suggest that these feedback processes had a crucial impact after 13.84 Ma during the final phase of global cooling and may have been instrumental in forcing the climate system across a crucial threshold. However, the scarcity of correlative records makes it difficult to assess the potential role of the EEP as a carbon sink in a global context and to evaluate to what extent equatorial productivity drove climate events and/or responded to global cooling during this fundamental climate transition.

CONCLUSION

Our study highlights the tight coupling of high- and low-latitude climate systems and the dynamic role of the EEP as a climate regulator through the Middle Miocene transition. During the later part of the MCO (16–14.7 Ma), transient shoaling of the carbonate compensation depth and enhanced carbonate dissolution in the deep Pacific Ocean coincided with episodes of peak warmth at Southern Hemisphere insolation maxima. These extreme events did not coincide with increased opal accumulation, indicating that EEP upwelling activity was either suppressed or limited by nutrient availability during global warming episodes. Two major increases in opal accumulation between ca. 14.0 and ca. 13.8 Ma support the notion that enhanced siliceous productivity and organic carbon burial in the EEP contributed to CO_2 drawdown, thus fostering global cooling.

ACKNOWLEDGMENTS

This research used samples provided by the Integrated Ocean Drilling Program and was funded by the Deutsche Forschungsgemeinschaft (grant HO233/1). We thank Ellen Thomas, Paul Wilson, and three anonymous reviewers for critical reviews.

REFERENCES CITED

Badger, M.P.S., Lear, C.H., Pancost, R.D., Foster, G.L., Bailey, T.R., Leng, M.J., and Abels, H.A., 2013, CO_2 drawdown following the middle Miocene expansion of the Antarctic Ice Sheet: Paleoceanography, v. 28, p. 42–53, doi:10.1002/palo.20015.

Chavez, F.P., and Barber, R.T., 1987, An estimate of new production in the equatorial Pacific: Deep-Sea Research, v. 34, p. 1229–1243, doi:10.1016/0198-0149(87)90073-2.

Dugdale, R.C., and Wilkerson, F.P., 1998, Silicate regulation of new production in the equatorial Pacific upwelling: Nature, v. 391, p. 270–273, doi:10.1038/34630.

Fedorov, A.V., Dekens, P.S., McCarthy, M., Ravelo, A.C., deMenocal, P.B., Barreiro, M., Pacanowski, R.C., and Philander, S.G., 2006, The Pliocene paradox (mechanisms for a permanent El Niño): Science, v. 312, p. 1485–1489, doi:10.1126/science.1122666.

Flower, B.P., and Kennett, J.P., 1994, The middle Miocene climatic transition: East Antarctic ice sheet development, deep ocean circulation and global carbon cycling: Palaeogeography, Palaeoclimatology, Palaeoecology, v. 108, p. 537–555, doi:10.1016/0031-0182(94)90251-8.

Holbourn, A.E., Kuhnt, W., Schulz, M., and Erlenkeuser, H., 2005, Impacts of orbital forcing and atmospheric CO_2 on Miocene ice-sheet expansion: Nature, v. 438, p. 483–487, doi:10.1038/nature04123.

Holbourn, A.E., Kuhnt, W., Schulz, M., Flores, J.-A., and Andersen, N., 2007, Middle Miocene long-term climate evolution: Eccentricity modulation of the "Monterey" carbon-isotope excursion: Earth and Planetary Science Letters, v. 261, p. 534–550, doi:10.1016/j.epsl.2007.07.026.

Laskar, J., Robutel, P., Joutel, F., Gastineau, M., Correia, A., and Levrard, B., 2004, A long term numerical solution for the insolation quantities of the Earth: Astronomy & Astrophysics, v. 428, p. 261–285, doi:10.1051/0004-6361:20041335.

Lawrence, K.T., Liu, Z., and Herbert, T.D., 2006, Evolution of the eastern tropical Pacific through Plio-Pleistocene glaciation: Science, v. 312, p. 79–83, doi:10.1126/science.1120395.

Lyle, M., Murray, D.W., Finney, B.P., Dymond, J., Robbins, J.M., and Brooksforce, K., 1988, The record of Pleistocene biogenic sedimentation in the eastern equatorial Pacific Ocean: Paleoceanography, v. 3, p. 39–59, doi:10.1029/PA003i001p00039.

Lyle, M., Dadey, K., and Farrell, J., 1995, The Late Miocene (11–8 Ma) eastern Pacific carbonate crash: Evidence for reorganization of deep-water circulation by the closure of the Panama Gateway, *in* Pisias, N.G., et al., Proceedings of the Ocean Drilling Program, Scientific results, Volume 138: College Station, Texas, Ocean Drilling Program, p. 821–838, doi:10.2973/odp.proc.sr.138.157.1995.

Lyle, M., Barron, J., Bralower, T.J., Huber, M., Olivarez Lyle, A., Ravelo, A.C., Rea, D.K., and Wilson, P.A., 2008, Pacific Ocean and Cenozoic evolution of climate: Reviews of Geophysics, v. 46, RG2002, doi:10.1029/2005RG000190.

Lyle, M., Olivarez Lyle, A., Gorgas, T., Holbourn, A., Westerhold, T., Hathorne, E., Kimoto, K., and Yamamoto, S., 2012, Data report: Raw and normalized elemental data along the Site U1338 splice from X-ray fluorescence scanning, *in* Pälike, H., et al., Proceedings of the Integrated Ocean Drilling Program, 320/321: Tokyo, Integrated Ocean Drilling Program Management International, Inc., doi:10.2204/iodp.proc.320321.203.2012.

Miller, K.G., Wright, J.D., and Fairbanks, R.G., 1991, Unlocking the ice house: Oligocene–Miocene oxygen isotopes, eustasy, and margin erosion: Journal of Geophysical Research, v. 96, p. 6829–6848, doi:10.1029/90JB02015.

Pälike, H., Lyle, M.W., Nishi, H., Raffi, I., Gamage, K., and Klaus, A., and the Expedition 320/321 Scientists, 2010, Proceedings of the Integrated Ocean Drilling Program, 320/321: Tokyo, Integrated Ocean Drilling Program Management International, Inc., doi:10.2204/iodp.proc.320321.109.2010.

Pälike, H., and 64 others, 2012, A Cenozoic record of the equatorial Pacific carbonate compensation depth: Nature, v. 488, p. 609–614, doi:10.1038/nature11360.

Philander, S.G., and Fedorov, A.V., 2003, Role of tropics in changing the response to Milankovich forcing some three million years ago: Paleoceanography, v. 18, 1045, doi:10.1029/2002PA000837.

Pichevin, L.E., Reynolds, B.C., Ganeshram, R.S., Cacho, I., Pena, L., Keefe, K., and Ellam, R.M., 2009, Enhanced carbon pump inferred from relaxation of nutrient limitation in the glacial ocean: Nature, v. 459, p. 1114–1117, doi:10.1038/nature08101.

Ragueneau, O., and 14 others, 2000, A review of the Si cycle in the modern ocean: Recent progress and missing gaps in the application of biogenic opal as a paleoproductivity proxy: Global and Planetary Change, v. 26, p. 317–365, doi:10.1016/S0921-8181(00)00052-7.

Rousselle, G., Beltran, C., Sicre, M.-A., Raffi, I., and De Rafélis, M., 2013, Changes in sea-surface conditions in the Equatorial Pacific during the middle Miocene–Pliocene as inferred from coccolith geochemistry: Earth and Planetary Science Letters, v. 361, p. 412–421, doi:10.1016/j.epsl.2012.11.003.

Shackleton, N.J., and Kennett, J.P., 1975, Paleotemperature history of the Cenozoic and the initiation of Antarctic glaciation: Oxygen and carbon analyses in DSDP Sites 277, 279, and 281, *in* Kennett, J.P., et al., eds., Initial reports of the Deep Sea Drilling Project, Volume 29: Washington, D.C., U.S. Government Printing Office, p. 743–755, doi:10.2973/dsdp.proc.29.117.1975.

Shevenell, A.E., Kennett, J.P., and Lea, D.W., 2008, Middle Miocene ice sheet dynamics, deep-sea temperatures, and carbon cycling: A Southern Ocean perspective: Geochemistry Geophysics Geosystems, v. 9, Q02006, doi:10.1029/2007GC001736.

Takahashi, T., Feely, R.A., Weiss, R.F., Wanninkhof, R.H., Chipman, D.W., Sutherland, S.C., and Takahashi, T.T., 1997, Global air-sea flux of CO_2: An estimate based on measurements of sea-air pCO_2 difference: National Academy of Sciences Proceedings, v. 94, p. 8292–8299, doi:10.1073/pnas.94.16.8292.

Vincent, E., and Berger, W.H., 1985, Carbon dioxide and polar cooling in the Miocene: The Monterey hypothesis, *in* Broecker, W.S., and Sundquist, E.T., eds., The carbon cycle and atmospheric CO_2: Natural variations Archean to present: American Geophysical Union Geophysical Monograph 32, p. 455–468.

Warny, S., Askin, A.R., Hannah, M.J., Mohr, B.A.R., Raine, J.I., Harwood, D.N., Florindo, F., and the SMS Science Team, 2009, Palynomorphs from a sediment core reveal a sudden remarkably warm Antarctica during the middle Miocene: Geology, v. 37, p. 955–958, doi:10.1130/G30139A.1.

Westberry, T., Behrenfeld, M.J., Siegel, D.A., and Boss, E., 2008, Carbon-based primary productivity modeling with vertically resolved photoacclimation: Global Biogeochemical Cycles, v. 22, GB2024, doi:10.1029/2007GB003078.

Winckler, G., Anderson, R.F., Fleisher, M.Q., McGee, D., and Mahowald, N., 2008, Covariant glacial-interglacial dust fluxes in the equatorial Pacific and Antarctica: Science, v. 320, p. 93–96, doi:10.1126/science.1150595.

Woodruff, F., and Savin, S., 1991, Mid-Miocene isotope stratigraphy in the deep sea: High resolution correlations, paleoclimatic cycles, and sediment preservation: Paleoceanography, v. 6, p. 755–806, doi:10.1029/91PA02561.

Manuscript received 2 July 2013
Revised manuscript received 10 September 2013
Manuscript accepted 10 September 2013

Printed in USA